

# Late Holocene increase of winter precipitation in mid-continental North America from a seasonally resolved speleothem record

Cameron J. Batchelor<sup>1</sup>, Shaun A. Marcott<sup>1</sup>, Ian J. Orland<sup>2</sup> and Kouki Kitajima<sup>1</sup>

<sup>1</sup>Department of Geoscience, University of Wisconsin–Madison, Madison, Wisconsin 53706, USA

<sup>2</sup>Wisconsin Geological and Natural History Survey, University of Wisconsin–Madison, Madison, Wisconsin 53705, USA

## ABSTRACT

Subannual climate reconstructions of the Holocene are rare despite the ability of such records to provide a better understanding of the underlying factors that drive subannual climate variability. We used specialized confocal laser fluorescent microscope imaging and automated secondary ion mass spectrometry microanalysis to resolve a seasonal oxygen isotope ( $\delta^{18}\text{O}$ ) record of a late Holocene-aged (2.7–2.1 ka) speleothem from mid-continental North America. We did this by measuring intra-band  $\delta^{18}\text{O}$  variability ( $\Delta^{18}\text{O}$ ) within 117 annual bands over a 600 yr span of the late Holocene. We interpret a change in  $\Delta^{18}\text{O}$  values after  $2.4 \pm 0.1$  ka to reflect an increase in the amount of winter precipitation. Our study produced direct measurements of past seasonality, offers new insights into shifting seasonal precipitation patterns that occurred during the late Holocene in central North America, and adds a new tool for understanding the complex precipitation and temperature histories of this region.

## INTRODUCTION

The climate of the Holocene is relatively well studied because of the availability of relevant climate archives and the importance of understanding Earth's most recent natural climate variability. Several large compilations of Holocene climate (Marcott et al., 2013; Wanner et al., 2015; Shuman and Marsicek, 2016; Kaufman et al., 2020) demonstrate clear millennial- to centennial-scale variability with both temporal and spatial complexity. Within these long-term records, seasonal climate reconstructions have become a focus of the paleoclimate community given the relevance to human time scales. But there are very few that span beyond the last  $\sim 1$  k.y. (Briffa, 2000; Pearl et al., 2020), limiting our understanding of long-term interannual Holocene climate variability. Developing more seasonal climate records over a larger portion of the Holocene is thus important for determining the most plausible underlying factors driving subannual variability. Here, we demonstrate one approach to filling this data gap by combining microimaging and microanalysis methods to report a seasonal-resolution record of oxygen

isotope ratios ( $\delta^{18}\text{O}$ ) for the first time in a North American speleothem.

Speleothems provide a unique opportunity for investigating past changes in seasonal climate. Their calcite layers can be precisely dated (Cheng et al., 2013), and the  $\delta^{18}\text{O}$  of speleothem calcite can record a signal of the  $\delta^{18}\text{O}$  of the precipitation ( $\delta^{18}\text{O}_{\text{precip}}$ ) above the cave (Lachniet, 2009), which provides the basis for interpreting past changes in climate. In some depositional settings, annual growth bands are identified in speleothems using confocal laser fluorescent microscopy (CLFM) (Orland et al., 2009). These annual growth layers, which can vary in thickness from micrometer to millimeter scale, can be manifested as fluorescent- and nonfluorescent-band couplets. Reconstructions of paleoseasonality from speleothems are increasing in the literature (Baldini et al., 2021) mainly because of gains in the sensitivity and spatial resolution of trace element analytical techniques. Seasonal records of  $\delta^{18}\text{O}$  from speleothems are still rare, however, because the practical spatial resolution of traditional drilling and micromilling sampling techniques required for isotope ratio mass

spectrometry are too coarse to resolve seasonal signals in most speleothems. We use secondary ion mass spectrometry (SIMS) in combination with CLFM imaging to measure  $\delta^{18}\text{O}$  *in situ* with 10- $\mu\text{m}$ -diameter analysis spots across 117 annual growth layers in a speleothem that grew from 2.7 to 2.1 ka in a mid-continental North American cave. These two methods provide direct measurements of past seasonality from speleothem growth layers that are only tens of micrometers thick (Orland et al., 2009, 2019) and resolve a seasonal climate signal during a snapshot of the late Holocene when multi-millennial moisture variability and climate were quickly changing in the study region (Shuman and Marsicek, 2016).

## Modern Cave Setting and Climatology

Stalagmite sample CM-4 (Fig. 1A) was collected from the upper Midwestern United States at Cave of the Mounds (Wisconsin; 43.0°N, 89.8°W, 450 m above sea level; Fig. 1B; Fig. S1 in the Supplemental Material<sup>1</sup>). This is a shallow cave setting (overburden of 10–15 m; Fig. S2), and observations indicate that this shallow setting allows for relatively instantaneous drip response to rain events. Cave of the Mounds is also a closed cave system with annually stable humidity and temperature (9 °C), which minimize concerns about the effects of kinetic fractionation. The cave is located in a region with strong seasonal climate where there are large differences between average winter (December–February;  $-7$  °C) and summer (June–August; 20 °C) temperatures (<https://www.iaea.org/services/networks/gnip/>, accessed 2021) (Fig. 2B). Modern precipitation totals amount to 830 mm/yr, with the majority (70%) accumulating during

<sup>1</sup>Supplemental Material. Extended methods, further discussion of the interpretation of fluorescent banding, and supplemental figures. Please visit <https://doi.org/10.1130/GEOL.S.19400918> to access the supplemental material, and contact [editing@geosociety.org](mailto:editing@geosociety.org) with any questions.

CITATION: Batchelor, C.J., et al., 2022, Late Holocene increase of winter precipitation in mid-continental North America from a seasonally resolved speleothem record: *Geology*, v. 50, p. 781–785, <https://doi.org/10.1130/G50096.1>

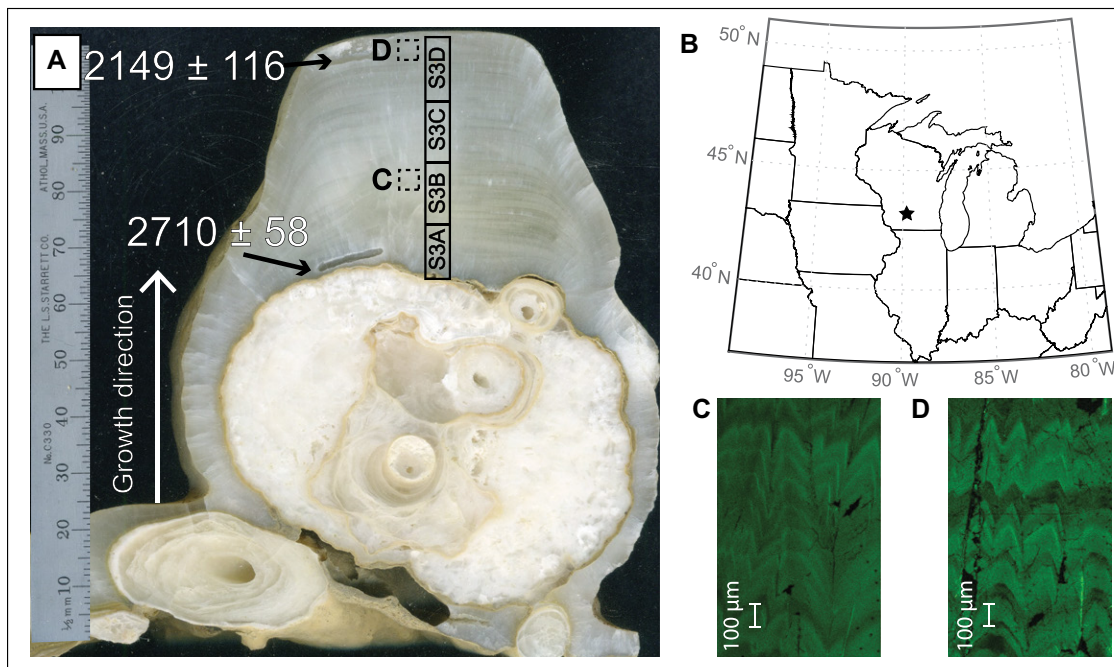


**Figure 1.** Cave of the Mounds (Wisconsin, upper Midwestern United States) stalagmite sample CM-4, location map, and fluorescent imaging. (A) Stalagmite sample CM-4 from Cave of the Mounds, showing U-Th ages (black arrows, in years before present [1950 CE]), growth direction (white arrow), and secondary ion mass spectrometry (SIMS) analysis areas (black boxes). Labeled areas inside the solid black boxes correspond to the location of SIMS sample mounts, which are shown in Figure S3 (see footnote 1). The dashed black boxes are areas in sample CM-4 where snapshot confocal laser fluorescent microscopy (CLFM) images (as shown in panels C and D) were taken. (B) Location of the Cave of the Mounds

(star). (C,D) Two examples of confocal laser fluorescent microscopy (CLFM) imaging showing fluorescent annual banding present in stalagmite CM-4. Note the entire growth axis of sample CM-4 was imaged using CLFM; location of images shown here is indicated by dashed boxes in A.

the spring (March–May) and summer (Fig. 2B). The oxygen isotope ratio of this precipitation ( $\delta^{18}\text{O}_{\text{precip}}$ ) exhibits a strong seasonal pattern, with the highest  $\delta^{18}\text{O}_{\text{precip}}$  values during the summer and the lowest values during the winter (https://www.iaea.org/services/networks/gnip/) (Fig. 2B). This seasonal pattern of  $\delta^{18}\text{O}_{\text{precip}}$  variability is primarily due to extreme temperature differences between the seasons, though other

interpretations exist, including seasonal shifts in moisture source and/or moisture recycling (Simpkins, 1995; Akers et al., 2017). Nonetheless, the strong seasonal climate regime of our field region along with the shallow and closed cave setting of Cave of the Mounds provide the basis of our interpretation that  $\delta^{18}\text{O}$  data within fluorescent couplets of stalagmite CM-4 reflect past variations in seasonal  $\delta^{18}\text{O}_{\text{precip}}$ .

## METHODS

Stalagmite sample CM-4 (Fig. 1A) was dated previously (Batchelor et al., 2019) and has two (top and bottom) U-Th ages of  $2149 \pm 116$  (two standard deviations [2 s.d.]) and  $2710 \pm 58$  (2 s.d.) yr B.P. (relative to 1950 CE) that were used to construct a linear age model. The entire length of the central growth axis was imaged by CLFM, which captured distinct fluorescent banding patterns. Fluorescence was stimulated with a 488-nm-wavelength laser, and a filter isolated emitted wavelengths between 505 and 539 nm (visible, green spectrum) on a Nikon A1RS Confocal Microscope at the University of Wisconsin–Madison (USA). After imaging, high-resolution  $\delta^{18}\text{O}$  analyses were completed on the CAMECA IMS 1280 large-radius multicollector ion microprobe (i.e., SIMS) at the WiscSIMS lab (Wisconsin Secondary Ion Mass Spectrometer Laboratory) at University of Wisconsin–Madison. We used a new automated sampling methodology established by the WiscSIMS lab that allowed the unattended analysis of samples using multiple software and programming packages (see the Supplemental Material). Applying these automated methods, we analyzed a total of 854 10- $\mu\text{m}$ -diameter pits approximately every 50  $\mu\text{m}$  along the central growth axis of sample CM-4. To reconstruct a seasonal climate signal, we also made multiple SIMS  $\delta^{18}\text{O}$  analyses ( $n = 2$ –10) across individual annual growth bands ( $n = 117$ ) and spatially referenced them using a microspatial database. The shallow pits that result from SIMS analysis were inspected by CLFM and established as being located within either a fluorescent (“bright”,

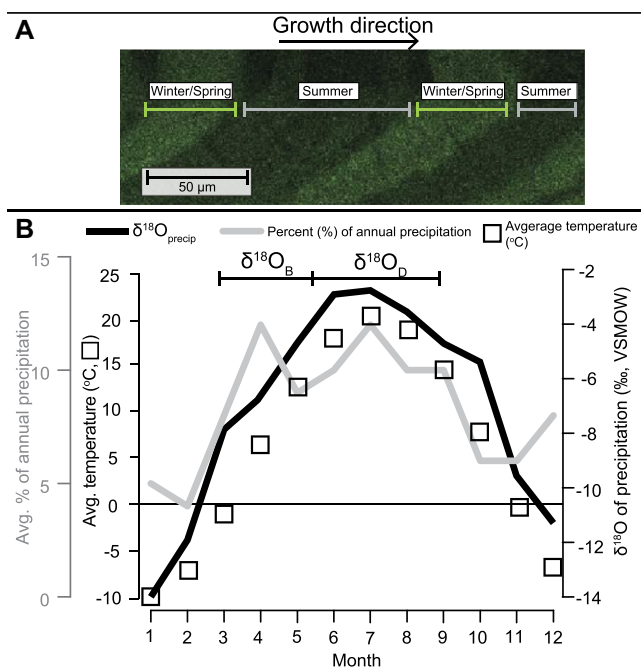


**Figure 2.** Fluorescent banding in speleothems and modern monthly climatology in the study region. (A) Confocal laser fluorescent microscopy (CLFM) image of sample CM-4 (from the Cave of the Mounds, Wisconsin, USA) fluorescent band couplets with the interpreted season of formation. (B) Monthly averages of percent of annual accumulated rainfall (gray line), average temperature ( $^{\circ}\text{C}$ ; black squares), and  $\delta^{18}\text{O}$  values of precipitation ( $\delta^{18}\text{O}_{\text{precip}}$ ; black line) from a precipitation monitoring site located in Chicago, Illinois, USA (https://www.iaea.org/services/networks/gnip/, accessed 2021). These data were collected over a ~20 yr period (1960–1979 CE). Interpreted season when the bright ( $\delta^{18}\text{O}_{\text{B}}$ )

and dark ( $\delta^{18}\text{O}_{\text{D}}$ ) fluorescent domains formed in stalagmite CM-4, as deduced from seasonal  $\delta^{18}\text{O}_{\text{precip}}$  differences, is also shown. VSMOW—Vienna standard mean ocean water.

$\delta^{18}\text{O}_B$ ) or nonfluorescent (“dark”,  $\delta^{18}\text{O}_D$ ) domain of the annual growth bands.

## RESULTS

The CLFM imaging revealed distinct fluorescent banding that ranged from 50 to 200  $\mu\text{m}$  thick along the entire central growth axis of sample CM-4 (Figs. 1C and 1D; Figs. S3A–S3D). A total of 841 individual SIMS  $\delta^{18}\text{O}$  measurements were made throughout sample CM-4 and ranged in value from  $-4.77\text{‰}$  to  $-7.92\text{‰}$  (all results reported on the Vienna Pee Dee belemnite [VPDB] scale) (Fig. 3A; Table S1 in the Supplemental Material). Of these analyses, a total of 442 were analyzed within 117 individual annual bands (Table S2). A total of 237 of these intra-band analyses were measured within bright domains ( $\delta^{18}\text{O}_B$ ; Fig. 3A, gray circles) and 205 were measured within dark domains ( $\delta^{18}\text{O}_D$ ; Fig. 3A, black triangles). Overall,  $\delta^{18}\text{O}_B$  values were lower than  $\delta^{18}\text{O}_D$  by  $0.25\text{‰}$ . We averaged all  $\delta^{18}\text{O}_B$  and  $\delta^{18}\text{O}_D$  values within each annual band and derived the difference ( $\Delta^{18}\text{O}$ ), which was used as a quantitative measure of seasonality. The average  $\Delta^{18}\text{O}$  value was  $-0.15\text{‰}$  for all annual bands in sample CM-4, and values ranged from  $+0.65\text{‰}$  to  $-1.61\text{‰}$  (Fig. 3B). To quantify the qualitative observation that seasonality changed across the sample’s growth period, we used a breakpoint analysis function to iden-

tify the separation between “older” and “younger” populations of  $\Delta^{18}\text{O}$  (see Fig. 3). The  $\Delta^{18}\text{O}$  values are lower in the younger part of the CM-4 record, illustrated by a shift in mean  $\Delta^{18}\text{O}$  from  $-0.05\text{‰}$  to  $-0.30\text{‰}$  at ca. 2.4 ka (Fig. 3B). We assign an uncertainty of  $\pm 0.1$  k.y. to the reported age of this shift (2.4 ka) as a conservative estimate consistent with the analytical precision of the bounding U-Th dates in our sample. Results of a Kolmogorov-Smirnov statistical test (Massey, 1951) as well as from a Monte Carlo bootstrapping simulation that we created (Fig. S4) indicate that the older and younger populations of  $\Delta^{18}\text{O}$  measured in annual bands of stalagmite CM-4 are statistically distinct ( $p < 0.05$ ; see the Supplemental Material).

## DISCUSSION

Several lines of evidence indicate that fluorescent couplets in sample CM-4 are likely annual and thus the  $\Delta^{18}\text{O}$  of these bands can be used to interpret past changes in seasonal climate. The first is the strong seasonal climate regime of the upper Midwestern United States that likely causes large seasonal variations of organic acid load carried by drip water given the shallow cave setting. We hypothesize that this seasonal cycle includes increased organic acid load during the spring thaw and decreased organic acid load in the continued rainy season

(summer) (see the Supplemental Material). This seasonal cycle has been observed in other studies that measured the dissolved organic content of surface waters in regions with seasonal climate patterns and vegetation similar to those of our field locality. These studies found the highest proportion of organic matter was present in surface waters during the spring thaw or during pronounced snowmelt events following the winter (Neff et al., 2006; Dalzell et al., 2007; Pellerin et al., 2012; Raymond et al., 2016) while summer surface waters had the lowest organic matter content (Dalzell et al., 2007). Together, these observations support the interpretation that fluorescent bands in sample CM-4 were formed annually.

To further test whether fluorescent couplets are annual, we compared the thickness of bands in sample CM-4 to their theoretical thickness based on our age model. The results of this test show a very strong match between measured (83  $\mu\text{m}$ ) and theoretical (80  $\mu\text{m}$ ) annual band thicknesses (Fig. S5). We therefore conclude that fluorescent laminations are likely annual in sample CM-4, that the sharp onset of bright domains formed from the first occurrence of springtime-water flushing of organic matter into the cave, and that subsequent dark domains formed predominantly during the summer (see Fig. 2A). This interpretation is supported by the observation that average  $\delta^{18}\text{O}_B$  values are less than average  $\delta^{18}\text{O}_D$  values in sample CM-4 (Fig. 3) because modern winter and spring  $\delta^{18}\text{O}_{\text{precip}}$  is lower than summer  $\delta^{18}\text{O}_{\text{precip}}$  (Fig. 2B). We note the smaller magnitude of  $\delta^{18}\text{O}$  variation between bright and dark calcite relative to seasonal  $\delta^{18}\text{O}_{\text{precip}}$  changes is likely due to groundwater mixing in the vadose zone. However, the fact that small, band-paced variations in  $\delta^{18}\text{O}$  are detected consistently through the sample suggests that a damped signal of seasonal  $\delta^{18}\text{O}_{\text{precip}}$  is preserved. We interpret relative changes in this  $\delta^{18}\text{O}$  signal to indicate changes in past seasonal rainfall  $\delta^{18}\text{O}$ .

Following a similar methodology as earlier studies (Orland et al., 2009, 2019), we interpret the difference in  $\delta^{18}\text{O}$  between the bright and dark domains within individual annual growth bands ( $\Delta^{18}\text{O} = \delta^{18}\text{O}_B - \delta^{18}\text{O}_D$ ) as a quantitative measure of seasonality. The intra-band analyses reveal that the average values of  $\Delta^{18}\text{O}$  in the older versus younger part of sample CM-4 are distinct and that  $\Delta^{18}\text{O}$  values in the younger population of annual bands (bands 71–117) are  $0.30\text{‰}$  lower than  $\Delta^{18}\text{O}$  values in the older population of annual bands (bands 1–70) (Fig. 3B). This apparent decrease in  $\Delta^{18}\text{O}$  is not aliased by annual band thickness (Fig. S5), thus we interpret this change in  $\Delta^{18}\text{O}$  to be climatically driven and that the occurrence of more-negative  $\Delta^{18}\text{O}$  values in the youngest part of sample CM-4 is likely a result of increased low- $\delta^{18}\text{O}$  wintertime precipitation.

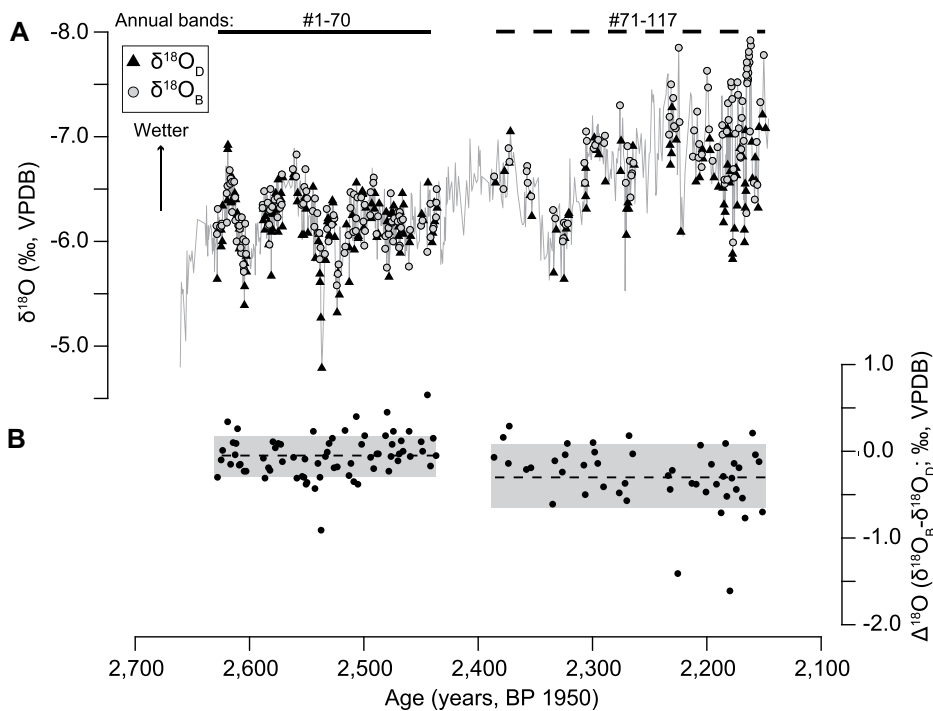


**Figure 3. Seasonal  $\delta^{18}\text{O}$  record for stalagmite CM-4 from the Cave of the Mounds (Wisconsin, USA) (panels A and B are on the same x-axis). (A)  $\delta^{18}\text{O}$  secondary ion mass spectrometry (SIMS) analyses for sample CM-4 (gray line) with labeled  $\delta^{18}\text{O}$  measurements of individual bright (gray circles;  $\delta^{18}\text{O}_B$ ) and dark (black triangles;  $\delta^{18}\text{O}_D$ ) fluorescent domains within individual annual growth bands. (B)  $\Delta^{18}\text{O}$  ( $\delta^{18}\text{O}_B - \delta^{18}\text{O}_D$ ) of each annual band, which is quantitative measure of seasonality. Average  $\Delta^{18}\text{O}$  values for “old” (bands 1–70) and “young” (bands 71–117) annual band populations, as distinguished by breakpoint analysis function, are shown (black dashed line) as well as two standard deviations (gray bar). VPDB—Vienna Pee Dee belemnite.**

These interpretations taken together suggest that the values of  $\Delta^{18}\text{O}$  in annual bands of sample CM-4 are representative of how wet past winters were, such that annual bands with the lowest  $\Delta^{18}\text{O}$  values reflect years with wetter winters than bands with the highest  $\Delta^{18}\text{O}$  values. As such, the decrease in  $\Delta^{18}\text{O}$  at  $2.4 \pm 0.1$  ka in the sample CM-4 record reflects an increase in the amount of winter precipitation at our field site (Fig. 3B). Nearby regional paleoclimate records, though not seasonal in resolution, also indicate that annual precipitation increased from 3 to 2 ka (Fig. 4B) (Shuman and Marsicek, 2016). Thus, we interpret that the younger part of the sample CM-4 record likely demonstrates a closer approximation of modern seasonality in the mid-continent of North America than the older part of the record which we interpret as recording drier winters. This is also consistent with other studies that inferred an increase in wintertime precipitation from the mid- to late Holocene at ca. 3 ka (Denniston et al., 1999; Anderson, 2012; Jiménez-Moreno et al., 2019).

## CONCLUSION

This study applies a combination of specialized imaging techniques and *in situ* micrometer-scale SIMS  $\delta^{18}\text{O}$  measurements in a Cave of the Mounds speleothem to produce a snapshot of seasonal paleoclimate dynamics in the mid-continent of North America during the late Holocene. The intra-band relationships between  $\delta^{18}\text{O}_B$  and  $\delta^{18}\text{O}_D$ , including lower  $\Delta^{18}\text{O}$  values in the youngest portion of sample CM-4, reveal there was an increase in winter precipitation from 3 to 2 ka. Further, our seasonally resolved record, when compared with other regional paleoclimate reconstructions (Fig. 4), suggests the winters in the upper Midwestern United States were likely drier at 3 ka than today and transitioned toward modern seasonality at  $2.4 \pm 0.1$  ka. These findings are corroborated by climate reconstructions from the western United States (Anderson, 2012; Jiménez-Moreno et al., 2019); however, our study refines existing work by providing the first direct measurements of past seasonality (*in situ*  $\delta^{18}\text{O}$  data across seasonal

stalagmite growth bands) in mid-continental North America as robust evidence that wintertime precipitation increased during this time. Although identifying a climate mechanism behind this seasonal change is out of the scope for this study, these results would be useful in exploring links between mid-continental seasonal climate and various climate modes (El Niño–Southern Oscillation, North Atlantic Oscillation, Pacific Decadal Oscillation) (Fye et al., 2006; Liu et al., 2011; Whan and Zwiers, 2017). We conclude by noting that this *in situ* approach could be used in other regional cave samples to further test our findings, given that there are several dated Holocene speleothems from the upper Midwestern region of the United States (see Batchelor et al., 2019).

## ACKNOWLEDGMENTS

This work was supported by the U.S. National Science Foundation (NSF) (grant P2C2-1805629 to S. Marcott and I. Orland) and the WiscSIMS Laboratory (K. Kitajima) which is supported by the NSF (grants EAR-1355590, EAR-1658823). We thank J. Klimczak and A. Wescott for their permission to collect stalagmite samples at Cave of the Mounds, Rich Slaughter for sample collection help, Drae Rogers for sample preparation, Lance Rodenkirch for CLFM help at the University of Wisconsin–Madison Optical Imaging Core, and Lawrence R. Edwards and associated colleagues for prior U-Th analyses at the University of Minnesota. Stalagmite CM-4 is curated at the University of Wisconsin–Madison Geology Museum. We thank Micheline Campbell and two anonymous reviewers for constructive comments that improved this manuscript, and Kathleen Benison for their editorial handling.

## REFERENCES CITED

- Akers, P.D., Welker, J.M., and Brook, G.A., 2017, Reassessing the role of temperature in precipitation oxygen isotopes across the eastern and central United States through weekly precipitation-day data: *Water Resources Research*, v. 53, p. 7644–7661, <https://doi.org/10.1002/2017WR020569>.
- Anderson, L., 2012, Rocky Mountain hydroclimate: Holocene variability and the role of insolation, ENSO, and the North American Monsoon: *Global and Planetary Change*, v. 92–93, p. 198–208, <https://doi.org/10.1016/j.gloplacha.2012.05.012>.
- Baldini, J.U.L., et al., 2021, Detecting and quantifying palaeoseasonality in stalagmites using geochemical and modelling approaches: *Quaternary Science Reviews*, v. 254, 106784, <https://doi.org/10.1016/j.quascirev.2020.106784>.
- Batchelor, C.J., Orland, I.J., Marcott, S.A., Slaughter, R., Edwards, R.L., Zhang, P., Li, X.L., and Cheng, H., 2019, Distinct permafrost conditions across the last two glacial periods in midlatitude North America: *Geophysical Research Letters*, v. 46, p. 13,318–13,326, <https://doi.org/10.1029/2019GL083951>.
- Briffa, K.R., 2000, Annual climate variability in the Holocene: Interpreting the message of ancient trees: *Quaternary Science Reviews*, v. 19, p. 87–105, [https://doi.org/10.1016/S0277-3791\(99\)00056-6](https://doi.org/10.1016/S0277-3791(99)00056-6).
- Cheng, H., et al., 2013, Improvements in  $^{230}\text{Th}$  dating,  $^{230}\text{Th}$  and  $^{234}\text{U}$  half-life values, and U-Th isotopic measurements by multi-collector inductively coupled plasma mass spectrometry: *Earth and Planetary Science Letters*, v. 371–372, p. 82–91, <https://doi.org/10.1016/j.epsl.2013.04.006>.

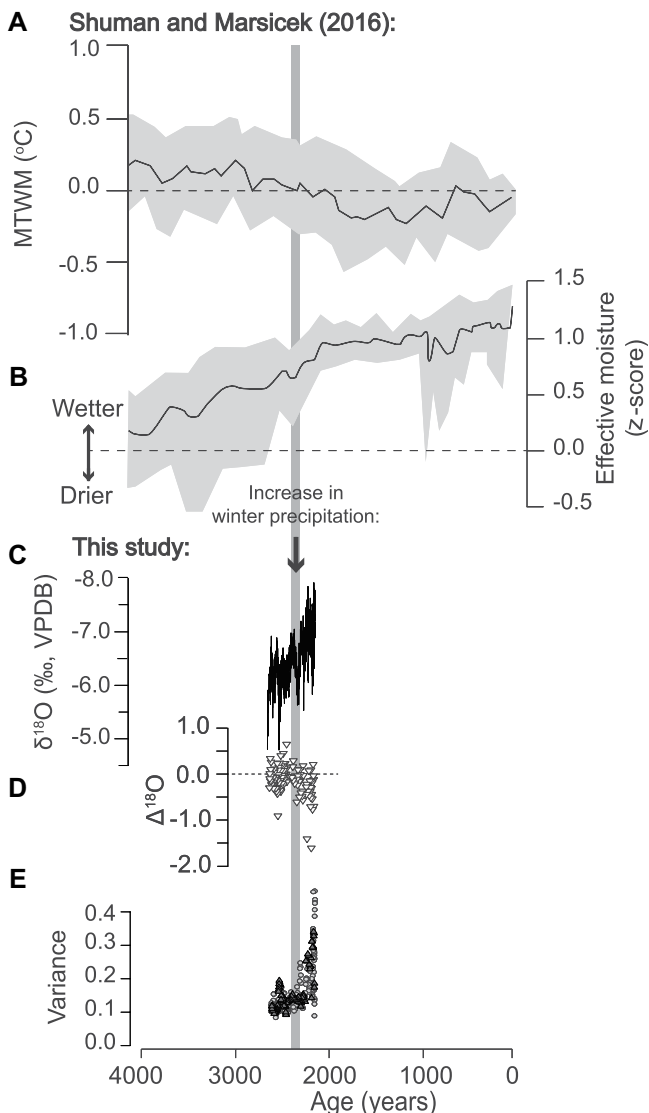


**Figure 4. Stalagmite CM-4 (from the Cave of the Mounds, Wisconsin, USA)  $\delta^{18}\text{O}$  record in context with regional paleoclimate records for the past 4 k.y. (A,B) Late Holocene trends in mean temperature of warmest month (MTWM) and effective moisture at several sites that span across the upper central-to-eastern United States (see Shuman and Marsicek, 2016). (C) Stalagmite CM-4  $\delta^{18}\text{O}$  record (this study) labeled with timing of the seasonal shift in moisture (ca. 2.4 ka; black arrow and vertical gray shading) as inferred from calculations of intra-band  $\delta^{18}\text{O}$  variability ( $\Delta^{18}\text{O}$ ; panel D). (D) Intra-band  $\delta^{18}\text{O}$  variability within annual bands of stalagmite CM-4 ( $\Delta^{18}\text{O}$ ). (E) Running-variance (every 10 data points) of  $\delta^{18}\text{O}_B$  (light gray) and  $\delta^{18}\text{O}_D$  (dark gray). Note the distinct increase in variance at ~2.4 ka. VPDB—Vienna Pee Dee belemnite.**

- Dalzell, B.J., Filley, T.R., and Harbor, J.M., 2007, The role of hydrology in annual organic carbon loads and terrestrial organic matter export from a mid-western agricultural watershed: *Geochimica et Cosmochimica Acta*, v. 71, p. 1448–1462, <https://doi.org/10.1016/j.gca.2006.12.009>.
- Denniston, R.F., González, L.A., Asmerom, Y., Baker, R.G., Reagan, M.K., and Bettis, E.A., III, 1999, Evidence for increased cool season moisture during the middle Holocene: *Geology*, v. 27, p. 815–818, [https://doi.org/10.1130/0091-7613\(1999\)027<0815:EFICSM>2.3.CO;2](https://doi.org/10.1130/0091-7613(1999)027<0815:EFICSM>2.3.CO;2).
- Fye, F.K., Stahle, D.W., Cook, E.R., and Cleveland, M.K., 2006, NAO influence on sub-decadal moisture variability over central North America: *Geophysical Research Letters*, v. 33, L15707, <https://doi.org/10.1029/2006GL026656>.
- Jiménez-Moreno, G., Anderson, R.S., Shuman, B.N., and Yackulic, E., 2019, Forest and lake dynamics in response to temperature, North American monsoon and ENSO variability during the Holocene in Colorado (USA): *Quaternary Science Reviews*, v. 211, p. 59–72, <https://doi.org/10.1016/j.quascirev.2019.03.013>.
- Kaufman, D., McKay, N., Routson, C., Erb, M., Dätwyler, C., Sommer, P.S., Heiri, O., and Davis, B., 2020, Holocene global mean surface temperature, a multi-method reconstruction approach: *Scientific Data*, v. 7, 201, <https://doi.org/10.1038/s41597-020-0530-7>.
- Lachniet, M.S., 2009, Climatic and environmental controls on speleothem oxygen-isotope values: *Quaternary Science Reviews*, v. 28, p. 412–432, <https://doi.org/10.1016/j.quascirev.2008.10.021>.
- Liu, Z.F., Kennedy, C.D., and Bowen, G.J., 2011, Pacific/North American teleconnection controls on precipitation isotope ratios across the contiguous United States: *Earth and Planetary Science Letters*, v. 310, p. 319–326, <https://doi.org/10.1016/j.epsl.2011.08.037>.
- Marcott, S.A., Shakun, J.D., Clark, P.U., and Mix, A.C., 2013, A reconstruction of regional and global temperature for the past 11,300 years: *Science*, v. 339, p. 1198–1201, <https://doi.org/10.1126/science.1228026>.
- Massey, F.J., Jr., 1951, The Kolmogorov-Smirnov test for goodness of fit: *Journal of the American Statistical Association*, v. 46, p. 68–78, <https://doi.org/10.1080/01621459.1951.10500769>.
- Neff, J.C., Finlay, J.C., Zimov, S.A., Davydov, S.P., Carrasco, J.J., Schuur, E.A.G., and Davydova, A.I., 2006, Seasonal changes in the age and structure of dissolved organic carbon in Siberian rivers and streams: *Geophysical Research Letters*, v. 33, L23401, <https://doi.org/10.1029/2006GL028222>.
- Orland, I.J., Bar-Matthews, M., Kita, N.T., Ayalon, A., Matthews, A., and Valley, J.W., 2009, Climate deterioration in the Eastern Mediterranean as revealed by ion microprobe analysis of a speleothem that grew from 2.2 to 0.9 ka in Soreq Cave, Israel: *Quaternary Research*, v. 71, p. 27–35, <https://doi.org/10.1016/j.yqres.2008.08.005>.
- Orland, I.J., He, F., Bar-Matthews, M., Chen, G.S., Ayalon, A., and Kutzbach, J.E., 2019, Resolving seasonal rainfall changes in the Middle East during the last interglacial period: *Proceedings of the National Academy of Sciences of the United States of America*, v. 116, p. 24,985–24,990, <https://doi.org/10.1073/pnas.1903139116>.
- Pearl, J.K., Anchukaitis, K.J., Donnelly, J.P., Pearson, C., Pederson, N., Gaylord, M.C.L., McNichol, A.P., Cook, E.R., and Zimmermann, G.L., 2020, A late Holocene subfossil Atlantic white cedar tree-ring chronology from the northeastern United States: *Quaternary Science Reviews*, v. 228, 106104, <https://doi.org/10.1016/j.quascirev.2019.106104>.
- Pellerin, B.A., Saraceno, J.F., Shanley, J.B., Sebestyen, S.D., Aiken, G.R., Wollheim, W.M., and Bergamaschi, B.A., 2012, Taking the pulse of snowmelt: *In situ* sensors reveal seasonal, event and diurnal patterns of nitrate and dissolved organic matter variability in an upland forest stream: *Biogeochemistry*, v. 108, p. 183–198, <https://doi.org/10.1007/s10533-011-9589-8>.
- Raymond, P.A., Saiers, J.E., and Sobczak, W.V., 2016, Hydrological and biogeochemical controls on watershed dissolved organic matter transport: Pulse-shunt concept: *Ecology*, v. 97, p. 5–16, <https://doi.org/10.1890/14-1684.1>.
- Shuman, B.N., and Marsicek, J., 2016, The structure of Holocene climate change in mid-latitude North America: *Quaternary Science Reviews*, v. 141, p. 38–51, <https://doi.org/10.1016/j.quascirev.2016.03.009>.
- Simpkins, W.W., 1995, Isotopic composition of precipitation in central Iowa: *Journal of Hydrology (Amsterdam)*, v. 172, p. 185–207, [https://doi.org/10.1016/0022-1694\(95\)02694-K](https://doi.org/10.1016/0022-1694(95)02694-K).
- Wanner, H., Mergel, L., Grosjean, M., and Ritz, S.P., 2015, Holocene climate variability and change: A data-based review: *Journal of the Geological Society*, v. 172, p. 254–263, <https://doi.org/10.1144/jgs2013-101>.
- Whan, K., and Zwiers, F., 2017, The impact of ENSO and the NAO on extreme winter precipitation in North America in observations and regional climate models: *Climate Dynamics*, v. 48, p. 1401–1411, <https://doi.org/10.1007/s00382-016-3148-x>.

Printed in USA